Comparison of measured and modeled outgoing longwave radiation for clear-sky ocean and land scenes using coincident CERES and AIRS observations

L. A. Moy,[1] R. O. Knuteson,[1] D. C. Tobin,[1] H. E. Revercomb,[1] L. A. Borg,[1] and J. Susskind[2]

Received 30 June 2009; revised 19 January 2010; accepted 5 March 2010; published 10 August 2010.

[1] Clear-sky outgoing longwave radiation (OLR) is computed using the Atmospheric and Environmental Research (AER), Inc., Rapid Radiative Transfer Model (RRTM) for comparison with the observations of the Clouds and the Earth's Radiant Energy System (CERES) for both ocean and land scenes. CERES clear-sky OLR is in agreement with RRTM model calculations to 0.2% accuracy using best estimate radiosondes (BE) launched coincident with NASA Aqua overpasses at the Atmospheric Radiation Measurement Southern Great Plains (SGP) site and 0.8% using retrieved profiles of temperature, water vapor, ozone, and surface parameters from the Atmospheric Infrared Sounder (AIRS) on the Aqua platform. A partial flux analysis using AIRS radiances implies an accuracy for the RRTM model in the far infrared of 0.4% (about 0.5 W/m^2) for wave numbers less than 650 cm^{-1} (wavelengths greater than 15.4 μm). CERES minus model biases over clear-sky ocean are similar to previously published results. Ordering the results according to the magnitude of the measured minus model mean bias for nighttime, tropical, ocean gives: +0.57 ± 1.9 W/m^2 (Dessler/Fu-Liou), +0.83 ± 1.5 W/m^2 (Huang/MODTRAN5), +1.6 ± 1.6 W/m^2 (Moy/RRTM), +3.7 ± 2.1 W/m^2 (Dessler/Chou). Comparison of observed minus modeled OLR over land are included in this study. Excluding nonfrozen ocean, a mean difference over land of +2.0 W/m^2 for nighttime cases and +1.0 W/m^2 for daytime cases is found where the land classes are weighted inversely by their standard error. The nighttime bias is quite consistent across all the land classes. The daytime bias shows less consistency with a tendency toward larger CERES minus AIRS RRTM OLR bias for the land classes with smaller vegetation fraction. Comparison of clear-sky CERES and AIRS RRTM OLR over cold snow-/ice-covered surfaces (mainly in the polar regions) is complicated by the use of the MODIS cloud mask in the identification of the clear CERES footprints used in the comparison. Clear scenes over cold surfaces can be identified more reliably in the daytime, for which the comparison between CERES and AIRS RRTM is better than 1.2 W/m^2 indicating good agreement.

Citation: Moy, L. A., R. O. Knuteson, D. C. Tobin, H. E. Revercomb, L. A. Borg, and J. Susskind (2010), Comparison of measured and modeled outgoing longwave radiation for clear-sky ocean and land scenes using coincident CERES and AIRS observations, *J. Geophys. Res.*, *115*, D15110, doi:10.1029/2009JD012758.

1. Introduction

[2] The earth's radiant energy budget is a balance between absorbed solar radiation and emitted outgoing longwave radiation (OLR). For almost 50 years now, accurate, long-term records of solar irradiance, planetary albedo, and OLR have been collected to monitor climate change. The first Earth radiation budget measurements were made by instruments built at the University of Wisconsin beginning in 1959 immediately following the International Geophysical Year and led to a downward revision of the computed Earth albedo to about 30% in the "darker" tropics [*House*, 1985; *Vonder Haar and Suomi*, 1971]. Estimates of the flux errors in these pioneering measurements were on the order of 10 W/m^2. The second generation of Earth radiation budget measurements came from the ESSA and Nimbus series of NASA satellites in the mid to late 1960s that flew medium resolution scanning radiometers [*Vonder Haar and Suomi*, 1971]. In the 1970s, the National Aeronautics and Space Administration (NASA) initiated the Earth Radiation and Budget Experiment (ERBE) to create a long-term climate record of the flow of radiation at the top of the atmosphere, for clear-sky and all sky

[1]Space Science and Engineering Center, University of Wisconsin-Madison, Madison, Wisconsin, USA.
[2]Laboratory for Atmospheres, NASA Goddard Space Flight Center, Greenbelt, Maryland, USA.

Copyright 2010 by the American Geophysical Union.
0148-0227/10/2009JD012758

conditions. The first generation of satellite radiometers in the ERBE program flew wide-field of view, flat-plate radiometers and narrow field-of-view scanning radiometers [*Barkstrom et al.*, 1989]. These instruments, launched in the mid 1980s, with greatly improved spatial resolution, have led to better estimates of the effect of clouds on the radiation budget [*Harrison et al.*, 1990]. Monthly mean flux errors were reduced to between 5 and 10 W/m^2. The Clouds and the Earth's Radiant Energy System (CERES) experiment, part of NASA's Earth Observing System (EOS) begun in the 1990s, has continued the ERBE measurements with a mission to improve the understanding of natural and human-induced global change [*Wielicki et al.*, 1995]. With its improved angular sampling and cloud classification CERES has further reduced error in the mean shortwave and longwave top-of-atmosphere fluxes [*Wielicki et al.*, 1998].

[3] In addition to measurements of OLR from broadband radiometers onboard satellites such as CERES, OLR is calculated with radiative transfer models (RTM) requiring atmospheric profile and surface properties as inputs. Measurements of OLR are preferred to model calculations, however the latter method is able to simulate the radiant energy flow throughout the atmosphere and offer information about the sensitivity to atmospheric constituents and surface properties. Also if the NASA Atmospheric Infrared Sounder (AIRS) hyperspectral radiance information and retrievals are used, inferences to errors in the spectroscopic line parameter database for the far infrared (i.e., wavelengths longer than 15 μm) can be made. This is important because the region is not as well validated. Closure experiments are difficult because the atmosphere is opaque to the far infrared from most ground-based observing stations and there are few spectrally resolved radiometers for the far infrared.

[4] This paper compares clear-sky OLR from the CERES instrument observations on the NASA Aqua platform to modeled values computed from the Atmospheric and Environmental Research (AER), Inc. Rapid Radiative Transfer Model (RRTM) using in situ observations from special radiosonde launches and satellite retrievals from the NASA AIRS instrument. The observed minus modeled comparison is performed first at the Department of Energy (DOE) Atmospheric Radiation Measurement (ARM) program Southern Great Plains (SGP) site where accurate in situ and remote measurements of the atmosphere and surface are available. Computations using AIRS profiles are extended over the ocean for comparison to previous studies [*Dessler et al.*, 2008; *Huang et al.*, 2008]. Finally observed minus modeled OLR comparisons over land are presented using the International Geosphere-Biosphere Programme (IGBP) land classification scheme to assist in interpreting the results.

[5] The following sections describe the relevant radiative transfer theory (Section 2), data and methods used in this study (Section 3), results (Section 4) and conclusions (Section 5).

2. Radiative Transfer Model

[6] AER, Inc. has developed the RRTM which uses a correlated-k method for radiative transfer based on prior calculations [*Mlawer et al.*, 1997]. The RRTM can be used to calculate shortwave fluxes, longwave fluxes and cooling rates at any level in 16 wave bands. Due to it's speed and accuracy, the RRTM model is widely used by the numerical weather prediction community (e.g., ECMWF, NCEP, GFS, WRF, MM5), and the climate community (e.g., ECHAM5) [*Iacono et al.*, 2000; *Morcrette*, 2001]. The RRTM model uses the line-by-line radiative transfer model (LBLRTM), primarily developed with support from the DOE ARM program, to provide the reference calculations from which top of atmosphere fluxes are computed via a rapid algorithm [*Clough et al.*, 1992, 2005; *Rothman et al.*, 2005]. Uncertainties in the spectroscopic line parameter databases used by line-by-line models and in the physics of line mixing and continuum contributions introduces uncertainties in the computed transmittances and radiances for every RTM [*Tjemkes et al.*, 2003]. The spectroscopy used in LBLRTM has been validated using University of Wisconsin airborne and ground-based Fourier Transform Spectrometers over the past 20 years [*Clough et al.*, 2005; *Tjemkes et al.*, 2003; *Revercomb et al.*, 1988]. A series of ground-based closure experiments have been conducted at the ARM sites evaluating both the model inputs (e.g., atmospheric state) and the comparison to the ground based AERI downwelling radiances [*Tobin et al.*, 1999; *Revercomb et al.*, 2003; *Turner et al.*, 2004; *Knuteson et al.*, 2004]. The ARM program supports ongoing activity at the SGP site for the validation of the spectroscopic line parameter database in the far infrared (i.e., wavelengths longer than 15 μm) and the water vapor continuum. Early observations of the rotational water vapor band from the ground-based Extended Range AERI in the arctic have lead to improvements in the far infrared H_2O continuum and line widths, however additional experiments are underway to further constrain the uncertainties in this important spectral region [*Tobin et al.*, 1999]. The RRTM has a stated clear-sky error of less than 1.0 W/m^2 relative to LBLRTM in total longwave net flux (10–3000 cm^{-1}) at any altitude [*Mlawer et al.*, 1997]. RRTM version 3.0 and LBLRTM version 10.4 are used in this study.

3. Data and Methods

3.1. CERES

[7] The CERES sensor was launched onboard the EOS Aqua spacecraft in May 2002. Two CERES instruments on the same platform allow for coincident cross-track and biaxial scan mode operations. Cross-track operation is used to sample over a large spatial extent and to continue ERBE-like measurements. The biaxial scan mode operation is used to take measurements at a wide range of viewing angles to improve the accuracy of angular distribution models (ADMs), which are needed to translate radiances to fluxes. Each CERES instrument has three channels - a shortwave (SW) channel (0.2–5 μm) to measure reflected sunlight, a 8–12 μm "window" region (WN) channel to measure Earth-emitted thermal radiation, and the total channel (0.2–100 μm) to measure all wavelengths of radiation. CERES OLR is estimated as the total minus the shortwave radiation, which is a potential source of day - night bias [*Minnis and Khaiyer*, 2000; *Minnis et al.*, 2004].

[8] CERES observations have three main sources of error: instrument calibration and stability, insufficient sampling of the angular variations of radiation, and the inability to adequately sample the large diurnal variation of solar reflected and earth-emitted radiation. The CERES stability require-

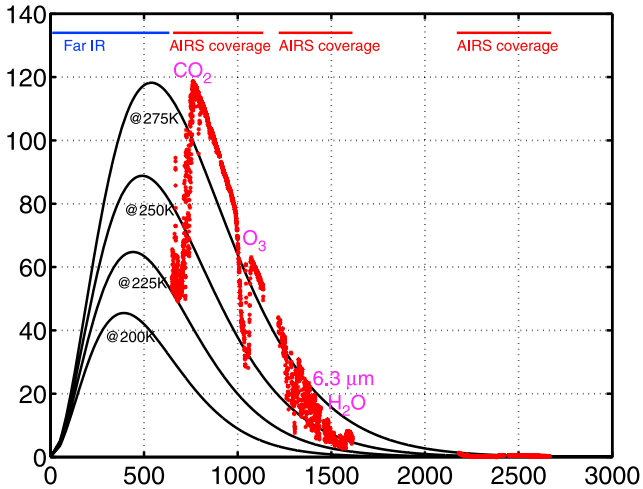

Figure 1. Illustration of the AIRS spectral coverage (shown in red) compared to Plank radiance curves as a function of wave number for a range of blackbody temperatures. The far infrared region, defined here to be wave numbers less than 650 cm^{-1}, contains the peak of atmospheric energy emission contributing to outgoing longwave radiation.

ment is 0.1% per year (0.5% over 5 years) for the total channel and 0.14% per year (0.7% over 5 years) for the SW channel. Because there are no direct methods of determining the instantaneous top-of-atmosphere (TOA) flux errors for a CERES footprint, published papers have focused on consistency tests that compare ADM-derived TOA fluxes of the same scene from different viewing angles. *Loeb et al.*'s [2007] paper specifically regarding EOS Terra CERES validation should also be applicable to the EOS Aqua CERES sensors. For all sky conditions, the overall instantaneous TOA flux error is estimated to be 3% (10 W/m^2 at the Terra overpass time) in the SW and 1.8% (3–5 W/m^2) in the LW.

[9] Our study uses the Single Scanner Footprint TOA/Surface Fluxes and Clouds (SSF) product CER_SSF_Aqua-FM3-MODIS_Edition 2B which contains one hour of instantaneous CERES data [*Geier et al.*, 2003]. The instantaneous data scene information in the CERES SSF product is derived partly from MODIS data. Scene identification including classification of surface classes and cloud properties are defined at the higher imager resolution and these data are averaged over the larger CERES footprint. The footprint at nadir viewing is approximately 20 km. SSF products include cloud information and CERES radiances for the total, SW, and window channels. The SW, LW, and WN radiances at the spacecraft altitude are converted to TOA fluxes.

3.2. Aqua AIRS

[10] Launched into a polar sun-synchronous orbit on 4 May 2002, the NASA EOS Aqua platform accommodates two broadband CERES instruments and the AIRS mid-infrared spectrometer [*Aumann et al.*, 2003]. The Aqua satellite is part of the "A-train" of NASA measurements which includes both passive and active remote sensing platforms. AIRS is the first of a new generation of satellite-based advanced infrared sounders, designed to provide data with higher vertical resolution and accuracy to numerical weather prediction centers for improved medium range weather forecasting [*Chahine et al.*, 2006; *Klaes et al.*, 2007; *Stockton et al.*, 2008]. *Aumann et al.* [2003, 2006] present an overview of the AIRS science objectives, data products, retrieval algorithms, and ground data processing concepts for the NASA EOS mission. Exploitation of the higher vertical resolution is made possible by high spectral resolution (resolving powers of about 1200) and the combined use of microwave and infrared radiances for the estimation of clear column radiance even in the presence of clouds [*Strow et al.*, 2006; *Chahine*, 1977; *Susskind*, 2007; *Susskind et al.*, 2006, 2010]. AIRS retrieval profiles of temperature and water vapor under clear and partly cloudy conditions are made for scenes with cloud fraction up to 90%. The AIRS infrared spectrometer acquires 2378 spectral samples in three spectral regions: 3.74 to 4.61 μm, 6.2 to 8.22 μm, and 8.8 to 15.4 μm. Figure 1 shows the region of the thermal infrared spectrum covered by the AIRS spectral channels. The spatial footprint size is 13.5 km at nadir, and cross track scanning provides twice daily global coverage. The AIRS Level 2 product files contain 6 min of data (240 files per day) with a 45 by 30 grid of fields-of-view with spacing of 50 km at nadir. Each set of 3 × 3 AIRS footprints is collocated with the Advanced Microwave Sounding Unit (AMSU) microwave footprint. The retrieved temperature, water vapor, and ozone profiles are reported in 100 pressure layers, the retrieved surface spectral emissivity is reported between 649 and 2664 cm^{-1} and a single surface temperature measurement is retrieved for the 50 km sounding region. Details of the retrieval algorithm are given by *Susskind et al.* [2003, 2006, 2010].

[11] The Goddard Earth Sciences Data Information and Services Center generates and distributes near real time geophysical parameters, including temperature and water vapor vertical profiles, ozone vertical profiles, surface emissivity spectra, and surface skin temperature, derived from coincident AIRS/AMSU observations using the AIRS Science Team retrieval algorithm [*Susskind*, 2007; *Susskind et al.*, 2010]. The results presented in this paper make use of Collection 5 (version 5) of the AIRS Level 2 products [*Susskind et al.*, 2010] and were obtained directly from the Goddard archive. The AIRS retrievals used in this study passed a number of data quality checks. Retrievals were included when QualSurf flags were less than 2 and PGood flags were greater than 700 hPa.

3.3. ARM Site

[12] Starting in the early 1990s the DOE ARM program has developed several ground sites around the world to collect detailed measurements of the atmospheric state and coincident radiation with an overall goal of improving the representation of radiation and clouds in climate models [*Stokes and Schwartz*, 1994]. The ARM Climate Research Facility ground sites have matured and are now well suited for providing data sets that are both accurately characterized and statistically significant for performing satellite validation [*Ackerman and Stokes*, 2003]. As part of a collaborative effort between the NASA EOS project and the ARM program, data from the heavily instrumented ARM sites are used to create "Best Estimates" of the atmospheric state and surface properties at the Aqua overpass times [*Tobin et al.*, 2006]. Combined with collocated AIRS observations, the

ARM products are being used for various studies, including assessment of clear-sky observed minus calculated radiance spectra, aimed at development and validation of the AIRS clear-sky forward RTM. Validation of the AIRS clear-sky radiative transfer algorithm using the ARM Best Estimate and other data are given by *Strow et al.* [2006]. *Tobin et al.* [2006] used the ARM site Best Estimate profiles to validate the AIRS Team temperature and water vapor retrievals for the tropical ocean site and the midlatitude land SGP site for all sky conditions. Whereas *Tobin et al.* [2006] provided validation of AIRS version 4, the current study uses AIRS version 5 products which includes improvements in Quality Control and in the retrievals over land.

3.4. Methodology

3.4.1. Model Validation

[13] To evaluate the accuracy of the RRTM model CERES observations are used as reference and to reduce the uncertainties in the inputted atmospheric state the ARM SGP Best Estimate profiles are used, as described by *Tobin et al.* [2006]. These Best Estimates of temperature and water vapor vertical profiles have known error characteristics which have been optimized for use with observations from the Aqua satellite using radiosondes with launch times just prior to and at Aqua overpass times. Since the ARM radiosonde data terminates near the tropopause, the Best Estimate temperature and water vapor profiles used in this study are appended above 70 mbar with the European Center for Medium Range Weather Forecasting (ECMWF) model output. A temperature correction based on Michelson Interferometer for Passive Atmospheric Sounding (MIPAS) comparisons is applied to the ECMWF temperature profiles [*Dethof et al.*, 2004]. Above the ECMWF's top level of 0.1 mbar, the U.S. standard profile is appended to 120 km. The RRTM calculations consider the seven major gases in the atmosphere: water vapor, carbon dioxide, ozone, nitrous oxide, carbon monoxide, and methane. The CO_2 concentrations are obtained from the NOAA database of measurements at the Mauna Loa Observatory in Hawaii. The ozone profile is set to match the U.S. Standard ozone profile shape with the total ozone column forced to agree with NASA's Total Ozone Mapping Spectrometer (TOMS) data set. The other trace gases are assumed to have the concentration of the U.S. standard profile [*U.S. Government Printing Office*, 1976]. For the Best Estimate RRTM calculations, upwelling LW ARM Best Estimate fluxes from a down-looking ground-based radiometer are converted to an effective surface temperature, with an assumed surface emissivity of '1'. The Surface flux values closest in time to the Aqua overpass times (within 30 min) are used. The CERES ARM Validation Experiment (CAVE) has made available a continuous record of CERES data at various sites [*Rutan et al.*, 2001; *Wielicki et al.*, 1996]. From the CAVE data set CERES SSF FM-3 data is subsetted within 10 km of the SGP site, 10 min of the Aqua overpass times, with satellite viewing angles less than 45 degrees, and with a 99% clear-sky requirement. Between September 2002 and March 2005, 127 RRTM calculations are matched to this CERES subset. The clear-sky CERES OLR at the ARM SGP site have an annual cycle with minima in the northern hemisphere winter near 220 W/m^2, and maxima in the summer near 320 W/m^2. There is also a marked day-night variation in OLR at the SGP site.

3.4.2. Model Input Assessment

[14] The Version 5 level 2 product retrieval of the NASA AIRS science team is used in this study for the global analysis using the RRTM model. This NASA AIRS product is available for both day and night, and over both ocean and land, so it is available for use in calculating a model comparison to nearly all of the clear CERES OLR measurements. The absolute accuracy of the AIRS retrieved temperature and water vapor profiles has been extensively studied as a function of atmospheric pressure and in the total column [*Tobin et al.*, 2006; *Divakarla et al.*, 2006; *McMillin et al.*, 2007; *Raja et al.*, 2008]. The sensitivity of calculated RRTM OLR to uncertainties in the input parameters has also been extensively studied by a number of authors [*Dessler et al.*, 2008; *Huang et al.*, 2007]. In this study the accuracy of the AIRS level 2 product is assessed relative to the ARM Best Estimate profiles. This is done by substituting the AIRS level 2 products for atmospheric temperature and water vapor, ozone, surface temperature and surface emissivity [*Strow et al.*, 2006; *Susskind*, 2007; *Susskind et al.*, 2010] in place of the ARM Best Estimate profiles as inputs into the RTM calculations used for the ARM SGP case study described in the previous section. AIRS emissivity is determined over the spectral interval between 3.75 and 15 microns via a physical retrieval methodology using a regression based first guess which is trained against laboratory emissivity spectra which cover this spectral region [*Susskind et al.*, 2010]. For AIRS RRTM calculations, the AIRS emissivity is spectrally averaged within 12 of the required 16 RRTM bands between 10 and 3250 cm^{-1}. Outside of the AIRS spectral regions, a value of unity is assumed. At frequencies lower than 650 cm^{-1}, very little surface emitted flux transmits to space, therefore, the emissivity assumption of unity outside the window regions does not affect computed OLR significantly. The same CERES clear-sky cases are used for comparisons with RRTM calculations using the AIRS level 2 products and ARM Best Estimate products as inputs to the RRTM.

[15] One potential source of inconsistency in this analysis is that the radiative transfer model used in the NASA AIRS science team retrieval is based on a custom line-by-line model developed for AIRS work that is adapted for use in a fast radiative transfer model whereas the RRTM model is based on LBLRTM [*Strow et al.*, 2006; *Clough et al.*, 2005]. OLR comparisons between RRTM calculations and CERES measurements provide a relative assessment of the AIRS profiles and the ARM Best Estimate profiles, but in terms of OLR flux (W/m^2) rather than state parameters.

[16] Another source of inconsistency in this analysis is the difference in the definitions of "clear sky" for CERES and AIRS data. CERES definition of clear sky uses the MODIS cloud flag. The intent of this clear criterion is to look between clouds in the so-called "clear-sky interstices." The potential problem with this detection method is contamination by small amounts of cloud, which would bias the "clear-sky" results toward the "all sky" results. On the other hand the AIRS level 2 product uses "cloud clearing" which uses a set of 3x3 fields of view to estimate the clear radiance component of the partly cloudy scene. This definition could bias the AIRS humidity result toward clear-sky conditions

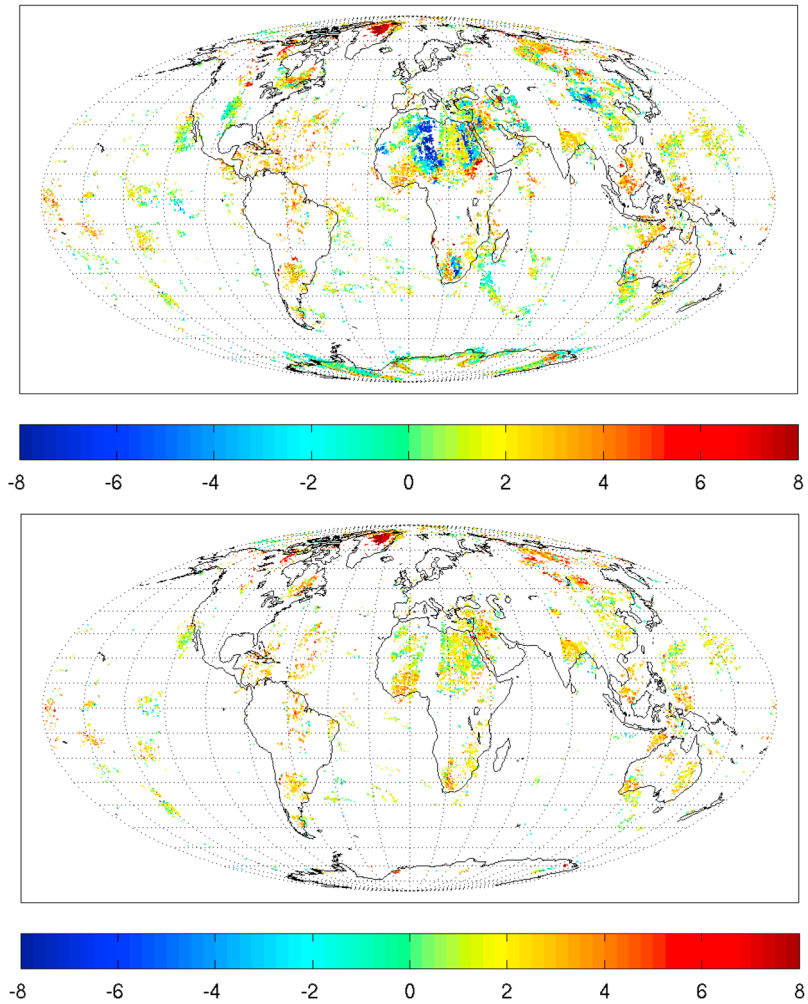

Figure 2. CERES-AIRS RRTM clear-sky OLR flux difference for 16 November 2002 in W/m^2 for (top) daytime/ascending and (bottom) nighttime/descending orbits.

and represent the true "all sky" humidity of the partly cloud scene. Our approach of collocating clear CERES fields of view to AIRS level 2 retrievals represents the conditions when the AIRS level 2 cloud cleared result should agree best with the CERES clear-sky product. Studies done by *Sohn and Bennartz* [2008] show that the contribution of different definitions of clear-sky to OLR differences is not negligible and are on the order of 2 W/m^2.

3.4.3. Modeled Versus Measured OLR: Nonfrozen Ocean

[17] In order to globally assess OLR differences between calculations from RRTM and measurements from CERES, four focus days were selected for clear-sky ocean and land scenes (16 November 2002, 18 February 2003, 5 May 2003, and 9 August 2003). Figure 2 shows the spatial coverage of the clear-sky CERES minus AIRS RRTM OLR comparison for one day. Figure 3 shows the latitude dependence of that difference for the same day. Differences are at a minimum near the equator and are largest at the poles. The accurate determination of clear-sky scenes over cold surfaces makes the AIRS/CERES comparison problematic at high latitudes. Related issues that require further investigation at high latitudes are the accurate determination of scene types, the knowledge of surface emissivity, and the retrieval of surface temperature inversions.

[18] The area covered by collocated CERES and AIRS footprints that are deemed clear is limited for any one day but the composite of all four days (day and night separately) provides reasonably good global coverage. Focus is first on the clear-sky ocean scenes for both day and night and statistics are computed for latitude zones comparable to previously published results. Results for modeled OLR using RRTM are compared to the results of the Fu-Liou and Chou models reported by *Dessler et al.* [2008] and the MODTRAN5 based radiance to flux conversion method reported by *Huang et al.* [2008]. This paper uses the same CERES and AIRS measurements as these reported studies noting that each study uses somewhat different time periods and spatial regions as well as different radiative transfer models. In this analysis, the CERES minus RRTM OLR differences are analyzed over the same time of day and latitude zones used in the published studies in order to draw conclusions about the systematic biases among the different radiative transfer models.

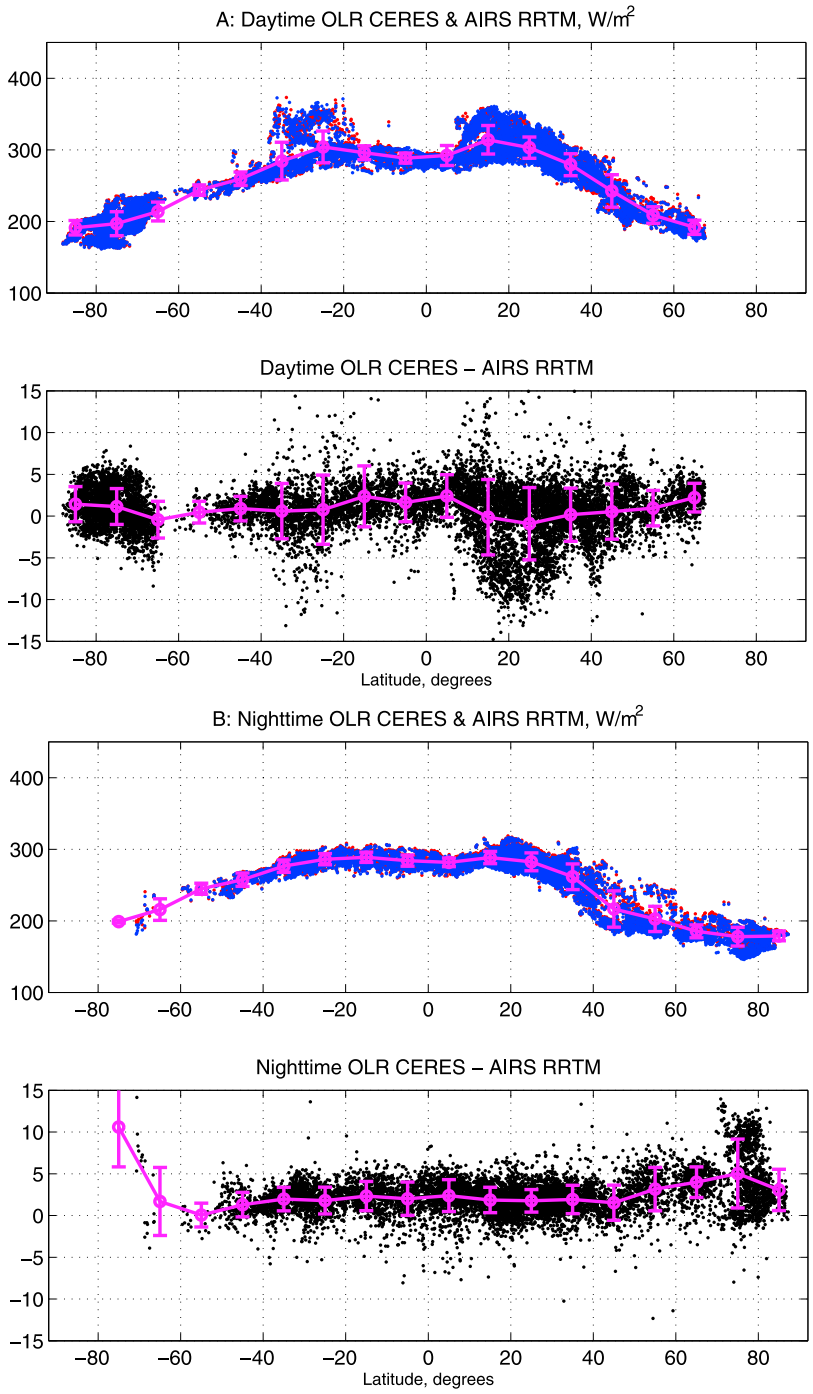

Figure 3. Latitude dependence of OLR for 16 Nov 2002 for (a) daytime/ascending and (b) nighttime/descending orbits for (top) clear-sky OLR and (bottom) CERES minus AIRS RRTM. CERES points are in red, AIRS RRTM are in blue. The means within 10 degree latitude bins with 1 standard deviation are also shown.

3.4.4. Modeled Versus Measured OLR: Land

[19] Unlike previous studies restricted to clear-sky ocean observations, this paper characterizes the comparison of modeled and measured OLR over land using AIRS retrieved temperature, water vapor, and ozone vertical profiles, and simultaneously retrieved surface skin temperature and surface spectral emissivity. Data analysis is performed according to the land classification scheme used by the CERES team, which is based upon the International Geosphere Biosphere Project (IGBP) classification [*Lambin and Geist*, 2006]. The evaluation against CERES OLR is one method of evaluating the consistency of the AIRS surface temperature and infrared emissivity product retrievals. The uncertainty in the AIRS surface skin temperature and surface emissivity has been previously evaluated by comparison to similar products produced by the NASA MODIS

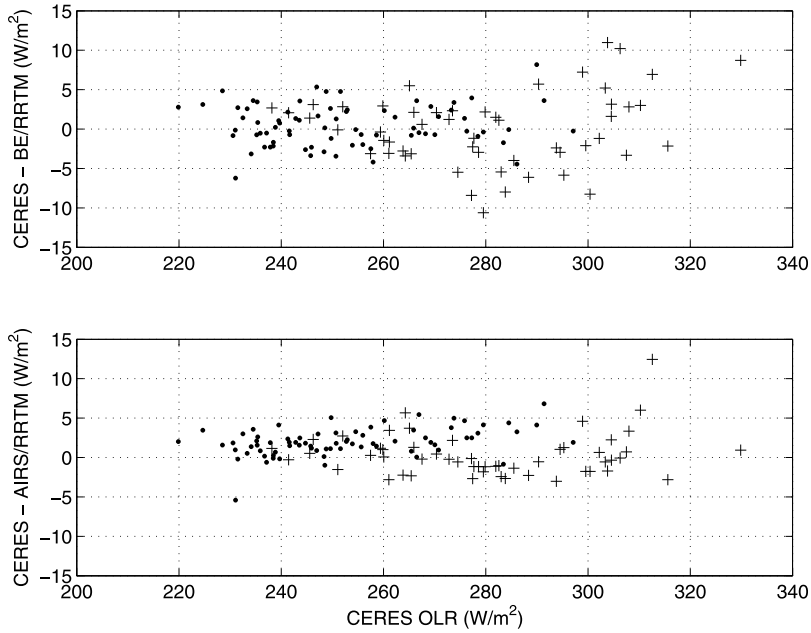

Figure 4. CERES comparison to (top) ARM Best Estimate OLR (labeled BE/RRTM) at the ARM SGP site and (bottom) OLR computed using AIRS profiles (labeled AIRS/RRTM). The pluses represent daytime cases, and the solid circles are the nighttime cases. The AIRS/RRTM OLR shows a significant day-night bias at the ARM SGP site. The CERES minus RRTM model results of the ARM SGP site validation are summarized in Table 1.

science team [*Wan*, 2008]. Results of the comparison by one of the coauthors of this paper are included in a recent report by the National Climate Data Center [*Pinheiro et al.*, 2008]. The error estimates of AIRS surface temperature and emissivity products are still under evaluation; however the relevant point for this work is that they are derived from AIRS radiances and used in a consistent manner to compute OLR. That is, the surface leaving radiance is the product of emissivity and Planck radiance at the skin temperature This results in errors that are correlated such that the surface leaving emission has higher accuracy than either the Planck radiance at the skin temperature or the emissivity individually. Of course the CERES measured OLR also contains uncertainties related to the use of radiance to flux conversion factors which could change with land class and season as well as uncertainty in the estimation of the LW flux during daytime from the difference of total minus SW flux. Thus the comparison of AIRS RRTM modeled and the CERES measured OLR provides insight into the land classes and times of day where good agreement can be expected and identifies classes which remain problematic for either AIRS or CERES. Included is a calculation of the sensitivity of OLR to the changes in the measured AIRS surface parameters over land to assist in the interpretation of the OLR comparison.

4. Results

4.1. Model Validation

[20] Figure 4 (top) shows a scatterplot of day and nighttime, clear-sky measurements of OLR by CERES versus clear-sky OLR calculated by the RRTM model driven by simultaneous measurements of atmospheric state contained in the Best Estimate product of *Tobin et al.* [2006] and described previously in Section 3.3. The Best Estimate RRTM calculations have larger scatter during daytime but both day and nighttime calculations are nearly unbiased relative to CERES measurements. Table 1 summarizes the

Table 1. Clear-Sky OLR Comparison at SGP[a]

OLR Differences: Observations − Calculations		CERES Mean (W/m^2)	Bias and Standard Deviation (W/m^2)	Number of Points	Uncertainty (k = 1) (W/m^2)	Day-Night Bias (W/m^2)
CERES − BE RRTM	Day	280.6	−0.05 ± 4.6	53	0.6	−0.55 ± 0.7
	Night	252.6	+0.5 ± 2.6	74	0.3	
CERES − AIRS RRTM	Day	280.6	+0.3 ± 2.7	53	0.4	−1.7 ± 0.45
	Night	252.6	+2.0 ± 1.8	74	0.2	

[a]CERES minus RRTM calculations statistics for Best Estimate profiles (BE RRTM) and for AIRS profiles (AIRS RRTM).

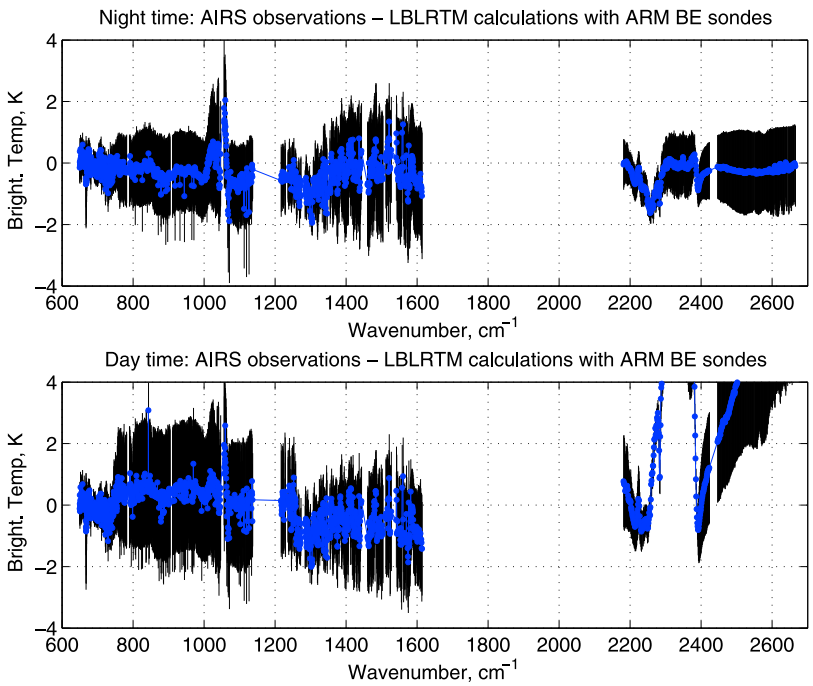

Figure 5. AIRS radiance observations - LBLRTM radiance calculations based on ARM Best Estimate profiles for the same subset of cases shown in Figure 4. (top) The nighttime cases and the (bottom) the daytime cases. The means are shown in blue with 1 standard deviation in black.

mean bias and uncertainty for the Best Estimate profiles used with RRTM. The CERES minus BE RRTM bias for day and night is consistent with zero within the 95% confidence level of the statistics. The relatively high accuracy of the ARM Best Estimate profiles allows us to conclude that the RRTM model is unbiased relative to CERES for clear skies to the level of 0.5 W/m^2 or less and thus to a percentage accuracy of 0.2%, since the mean calculated OLR for this validation set is 263 W/m^2.

[21] *Huang et al.* [2007] have made an estimate of the sensitivity of OLR to uncertainty in the spectroscopy of water vapor in the far infrared and concluded that the different representations of the water vapor continuum induce relatively small differences in OLR. This is relevant to the RRTM model because it is constructed using calculations of the LBLRTM line-by-line model which has used an evolving set of water vapor continuum representations validated against ground-based infrared observations [*Clough et al.*, 1989; *Tobin et al.*, 1999; *Turner et al.*, 2004; *Clough et al.*, 2005].

[22] The investigation of the implications of our OLR results on the far infrared spectroscopy contained in RRTM consisted of constraining the error in the middle infrared spectral region covered by the AIRS radiance observations. Spectral radiance calculations with the LBLRTM model were made using exactly the same Best Estimate profiles used in the BE RRTM calculation of OLR. The brightness temperature mean spectral difference, here defined as the AIRS radiance observations minus LBLRTM calculations using BE profiles, is shown in Figure 5. The observed minus calculated bias in the 6.3 μm water vapor band which differ between day and night by 0.5 to 1.0 K may be due to upper level water vapor radiosonde biases [*Miloshevich et al.*, 2006]. Systematic radiance calculation errors in the water

Table 2. Estimate of Percentage Uncertainty in the Far Infrared Contribution to RRTM Obtained by Comparison of the Measured Minus Modeled Error in the Total OLR to the Measured Minus Modeled Fractional Error in the Portion of the Midinfrared Covered by the AIRS Spectrum[a]

Spectral Range Definition	Mean Flux (W/m^2)	Coverage (%)	Percent Error Definition	Standard Error (k = 1)
Total IR (CERES LW)	263	100	(CERES OLR − BE RRTM OLR)/ CERES OLR	0.5 W/m^2, 0.2%
Middle IR (AIRS spectra 650–2700 cm^{-1})	144	54	(AIRS Radiance to Flux − BE LBLRTM Radiance to Flux)/ AIRS Radiance to Flux	0.4 W/m^2, 0.3%
Far Infrared (<650 cm^{-1})	116	45	Far IR estimate = Total − Mid IR	0.5 W/m^2, 0.4%

[a]The missing 1% of the total weight is due to coverage gaps in the AIRS spectrum. Estimates are based on CERES measurements at the ARM SGP site compared to modeled OLR using RRTM with input from the ARM Best Estimate profiles.

Table 3. Clear-Sky CERES Minus AIRS OLR for Nonfrozen Ocean Showing the Mean and Standard Deviation Within the Four Dates Included in the Analysis[a]

Author/Model/ Observation Date	Day-Night	20°N–20°S	30°N–30°S	30°N–70°N	70°S–30°S	70°S–70°N
Moy/RRTM/16 Nov.2002	Night	+2.2 ± 1.8 (288.2, 1825)	+2.0 ± 1.8 (288.4, 2612)	+1.3 ± 1.6 (272.5, 432)	+1.1 ± 1.3 (267.1, 561)	+1.8 ± 1.7 (283.1, 3605)
	Day	+2.0 ± 1.9 (291.9, 2113)	+1.7 ± 1.8 (292.6, 3277)	+1.5 ± 1.6 (275.6, 386)	+0.7 ± 1.5 (264.3, 1049)	+1.5 ± 1.8 (284.9, 4712)
Moy/RRTM/18 Feb. 2003	Night	+1.3 ± 1.4 (293.7, 3764)	+1.3 ± 1.4 (292.8, 4776)	+1.1 ± 1.6 (257.8, 568)	+0.7 ± 1.3 (268.4, 923)	+1.2 ± 1.4 (286.0, 6267)
	Day	+0.8 ± 1.7 (295.3, 3714,)	+0.9 ± 1.7 (293.8, 5357)	+1.4 ± 1.8 (259.4, 350)	+0.3 ± 1.6 (269.8, 1365)	+0.8 ± 1.7 (287.5, 7072)
Moy/RRTM/05May 2003	Night	+1.5 ± 1.7 (290.9, 3059)	+1.3 ± 1.6 (291.0, 4027)	+0.3 ± 1.3 (262.4, 722)	+1.0 ± 1.4 (268.1, 935)	+1.2 ± 1.6 (283.6, 5684)
	Day	+1.2 ± 1.8 (292.5, 2219)	+1.0 ± 1.8 (291.7, 3006)	+0.2 ± 1.7 (259.9, 611)	+1.5 ± 1.6 (270.5, 1382)	+1.0 ± 1.8 (282.0, 4999)
Moy/RRTM/09Aug 2003	Night	+1.2 ± 1.4 (292.2, 2400)	+1.3 ± 1.5 (290.4, 3481)	+1.1 ± 1.4 (284.9, 1468)	+0.5 ± 1.3 (261.1, 512)	+1.1 ± 1.5 (286.1, 5461)
	Day	+0.7 ± 1.6 (293.8, 2459)	+0.6 ± 1.6 (291.8, 3624)	+0.5 ± 1.7 (283.7, 909)	+0.3 ± 1.4 (263.4, 371)	+0.6 ± 1.6 (288.2, 4904)
Moy/RRTM/4 Day Mean/RSS	Night	+1.6 ± 1.6	+1.5 ± 1.6	+0.9 ± 1.5	+0.8 ± 1.3	+1.3 ± 1.5
	Day	+1.2 ± 1.7	+1.0 ± 1.7	+0.9 ± 1.7	+0.7 ± 1.5	+1.0 ± 1.7

[a]Unit is W/m^2. The four day mean and the root sum square of the standard deviations are also provided.

vapor band may also be due to errors in the water vapor line strengths and widths found in the HITRAN database [*Rothman et al.*, 2005; *Shephard et al.*, 2009]. However, these brightness temperature biases in the vibrational water vapor band are only a small error in the spectrally integrated flux due to the very small radiance values they represent. In order to convert the results to a percentage flux error the spectral mean radiance difference is integrated and divided by the integrated spectral radiance, assuming that the radiance to flux conversion factors divide out in the ratio. The result is given in Table 2 and shows that the spectral region covered by AIRS (which is 54% of the total OLR flux) is known to 0.4 W/m^2 or equivalently to 0.3% of the partial flux contributed by the middle infrared. Given that an estimate of the total flux error of RRTM from the Best Estimate comparison to CERES of 0.2%, a crude estimate of the uncertainty in the far infrared spectroscopy contained in the RRTM model can be made by taking the root sum square of the errors of the total flux and the middle infrared to obtain the value of 0.4% (0.5 W/m^2). This represents the maximum far infrared error contribution to the flux integral for wave numbers less than 650 cm^{-1} (or wavelengths greater than 15.4 μm). Given the paucity of direct observations in the far infrared this estimate is useful in guiding our interpretation of the results from the RRTM model since it rules out any large cancellation of errors occurring between the middle and far infrared spectroscopy [*Mlynczak et al.*, 2006].

4.2. Model Input Assessment

[23] Figure 4 (bottom) shows the comparison of AIRS LBLRTM calculations of OLR relative to CERES measurements for the same cases for which the ARM Best Estimate calculations of OLR (BE RRTM) were performed. Table 1 summarizes the results of the mean and standard deviation of the two sets of calculations relative to CERES measurements. CERES clear-sky OLR is in agreement with RRTM model calculations to within 1% accuracy using either BE profiles or AIRS retrievals. The AIRS RRTM standard deviation is considerably smaller than the Best Estimate RRTM. Replacing the Best Estimate point estimates of surface temperature and unit emissivity with the coincident AIRS skin temperature and emissivity retrieval has been shown to reduce the daytime variability in OLR difference to the same value as the CERES minus AIRS RRTM result. This suggests that attempting to match the CERES satellite footprints to surface point measurements introduces an additional sampling error into the comparison which is reduced when the similarly sized CERES and AIRS fields of view are used instead. The CERES minus AIRS RRTM results show a significant day night bias not seen in the sonde based Best Estimate RRTM comparison to the same CERES measurements. The day - night bias of −1.7 W/m^2 is twice as large as the uncertainty at the 95% confidence level. The daytime AIRS RRTM OLR calculations are in agreement with the CERES measurements within the standard error, however the nighttime AIRS RRTM calculations differ by 2.0 W/m^2 which is also well outside the statistical uncertainty. One possibility for the day - night bias is that AIRS can mistake a low cloud deck as the surface. The temperature contrast between the surface and a low cloud deck is greater in the day time making it less likely AIRS will mistake a cloud for the surface in the day.

Table 4. Clear-Sky CERES Minus AIRS OLR for Nonfrozen Ocean as Mean and Standard Deviation for the Indicated Latitude Zones[a]

Author Model Observation Date	Day-Night	20°N–20°S	30°N–30°S	30°N–70°N	30°S–70°S	70°N–70°S
Huang MODTRAN	Night	n/a	+0.83 ± 1.5	n/a	n/a	n/a
Jan–Dec 2004	Day	n/a	+0.62 ± 1.2	n/a	n/a	n/a
Dessler Fu-Liou	Night	+0.57 ± 1.9	n/a	−0.80 ± 2.9	−0.37 ± 2.0	−0.01 ± 2.1
March 2005	Day	n/a	n/a	n/a	n/a	n/a
Dessler Chou	Night	+3.7 ± 2.1	n/a	+3.7 ± 2.2	+3.3 ± 1.9	+3.7 ± 2.1
March 2005	Day	n/a	n/a	n/a	n/a	n/a
Moy RRTM	Night	+1.6 ± 1.6	+1.5 ± 1.6	+0.9 ± 1.5	+0.8 ± 1.3	+1.3 ± 1.5
4 Day Mean/RSS	Day	+1.2 ± 1.7	+1.0 ± 1.7	+0.9 ± 1.7	+0.7 ± 1.5	+1.0 ± 1.7

[a]Unit is W/m^2. The bias and standard deviation are included from *Huang et al.* [2007] and *Dessler et al.* [2008] for comparison with the results of this paper. The Dessler averages are computed first in 10 degree latitude bins and then weighted by area. The other results are not area-weighted.

Another possibility learned from line-by-line calculations with the AIRS profiles is that AIRS radiances in the 6.3 μm water vapor band are not being fit as well as the Best Estimate calculations shown in Figure 5. This may indicate a bias in the AIRS water vapor profile retrievals in the mid to upper troposphere which could explain the OLR bias. Note that errors of only 10% above 5 km can cause OLR errors of 1 W/m^2 or more and it is difficult to validate upper level water vapor profiles to this accuracy using conventional methods [*Dessler et al.*, 2008; *Miloshevich et al.*, 2006].

4.3. Modeled Versus Measured OLR: Nonfrozen Ocean

[24] Table 3 contains the summary of the clear-sky, ocean only CERES minus AIRS RRTM comparisons for the average of the four focus days used in this study. The statistics are computed over the same latitude zones used by previous authors to facilitate comparison with those results [*Dessler et al.*, 2008; *Huang et al.*, 2008]. The close agreement between daytime and nighttime bias and standard deviation for each latitude zone in the four day mean suggest that the sampling numbers within each zone are adequate. A bias in the range of 1.0 to 1.6 W/m^2 is found for the two definitions of tropical zones which decreases to about 0.8 W/m^2 for the midlatitude zones. The northern and southern midlatitude zone have nearly equal biases yielding a quite symmetric distribution of measured minus modeled flux errors about the equator which suggests that the average of the four focus days is capturing the annual average. In contrast the results of *Dessler et al.* [2008], shown in Table 4, exhibit a distinct north/south bias for the month of March 2005. This shift in error between northern and southern midlatitudes can also be seen in each of the four focus days studied in this paper. Compared here are the clear-sky measured minus model OLR for the four radiative transfer models presented by *Huang et al.* [2008], *Dessler et al.* [2008], and this paper. Only the nighttime results over the tropical ocean can be directly compared among all four models, as seen in Table 4. Ordering the results according to the magnitude of the measured minus model mean bias for nighttime, tropical, ocean gives: +0.57 ± 1.9 (Dessler/Fu-Liou), +0.83 ± 1.5 (Huang/MODTRAN5), +1.6 ± 1.6 (Moy/RRTM), +3.7 ± 2.1 (Dessler/Chou).

[25] Provided next is an interpretation of these results and the implications for models and model input. It should be first noted that the CERES and model comparisons shown here are each within the uncertainty of the input parameters as shown in previous sensitivity studies. However, the use of the same CERES measurement set in the comparison of these models provides a common reference that facilitates interpretation of the models results and also of the models inputs. In the comparison of the Huang/MODTRAN5 results to the results of this paper (Moy/RRTM), the Moy/RRTM bias is about +0.8 W/m^2 larger, i.e., AIRS OLR is lower in the Moy/RRTM results than the Huang/MODTRAN5 results. Since RRTM and MODTRAN5 are created using similar versions of the AER LBLRTM model and HITRAN database, it can be inferred that the difference is mainly due to model input. [*Clough et al.*, 2005; *Berk et al.*, 2005; *Huang et al.*, 2008]. Decreasing the AIRS water vapor profiles by 10% above 5 km to the input model profiles makes the LBLRTM computed radiances agree with the AIRS observed radiances. Using these adjusted profiles as input into the RRTM brings Huang/MODTRAN5 and Moy/RRTM into better agreement. The reason the Huang/MODTRAN5 analysis obtains a consistent water vapor amount with AIRS? is that the method used is a regression between simulated radiances using MODTRAN5 and temperature and water vapor profiles which is then applied directly to the AIRS radiances. The AIRS science team level 2 products are not used in the Huang/MODTRAN5 analysis, which makes it an independent way of estimating the AIRS OLR in a manner that is closely consistent with the relevant version of the LBLRTM/HITRAN version used to create MODTRAN5 and RRTM. The relative comparison of Huang/MODTRAN5 and Moy/RRTM suggests a bias in the AIRS level 2 upper level water vapor products used in this study as input to the RRTM model. This conclusion is also consistent with the results at the ARM SGP site discussed in section 4.2.

[26] Table 4 includes a comparison of the results of this paper to the measured minus modeled OLR presented by *Dessler et al.* [2008]. The method used by *Dessler et al.* [2008] is very similar to that used in this paper; the same clear-sky CERES data set is used as well as the same AIRS level 2 product version. The first key difference is the time period of the comparison, Dessler results are for 31 days but only for a single month (March 2005) while this paper uses only four days but selected to sample the seasonal cycle. The second key difference is the radiative transfer models used; *Dessler et al.* [2008] present a comparison of the Fu-Liou and Chou models while this paper uses the RRTM model. Any bias in the input profiles from the AIRS level 2 science team product are expected to be common between this paper and the *Dessler et al.* [2008] results, therefore the observed sys-

tematic difference is likely a model bias between RRTM and the Fu-Liou or Chou models. For clear-sky, nighttime, tropical ocean, scenes the CERES measured minus RRTM modeled OLR is 1.0 W/m^2 higher than the Fu-Liou model but 2.1 W/m^2 below the same results for the Chou model. Attributing these biases to model systematic errors leads to the following conclusions; the Chou model predicts a lower OLR than RRTM by 2.1 W/m^2 and RRTM predicts a lower OLR than Fu-Liou by 1.0 W/m^2. *Dessler et al.* [2008] suggest that the range of OLR calculations represented by Fu-Liou and Chou models is consistent with estimates of about 1% uncertainty in the model fluxes due to the approximations used in radiative transfer models [*Chou et al.*, 2001; *Briegleb*, 1992]. Since the RRTM model results fall between the Chou and Fu-Liou results, the agreement of better than 1% accuracy of the models for clear sky is confirmed; however our validation results for RRTM at the ARM SPG site imply an RRTM accuracy relative to CERES of about 0.2%. This work suggests that further effort for the validation of OLR radiative transfer models in clear-sky conditions is warranted and, through careful use of CERES and ground-truth data, should reduce the relative error among these models.

4.4. Modeled Versus Measured OLR: Land

[27] Global CERES minus AIRS RRTM OLR comparisons are analyzed by CERES surface land classes. Excluding non-frozen ocean, a difference over land is found of +2.0 W/m^2 for nighttime cases and +1.0 W/m^2 for daytime cases, where the land classes are weighted inversely by their standard error. The source of this global day-night difference becomes clearer when the land classes are considered in detail. The forest classes (1 to 5) show little day-night bias, noting that these classes are high emissivity scenes with relatively small seasonal variability. Excluding snow and ice classes, the day - night bias increases as the average vegetation fraction decreases from forested classes, through savanna to shrubland, croplands, grassland, and finally deserts.

[28] The nighttime CERES measurements of OLR avoid the complications of the SW contribution to the total flux and consistency between CERES and AIRS RRTM OLR is expected and is in fact the case for most land classes at night. The barren/desert class 16 is a land classification for which the nighttime CERES minus AIRS RRTM OLR difference is a very reasonable 1.1 W/m^2, but the daytime difference is −5.0 W/m^2. This result could be explained by errors in the modeling of the outgoing radiation from these surfaces, i.e., skin temperature and surface emissivity for AIRS retrievals and/or in the flux estimation over land for CERES measurements.

[29] A mean difference between the day and night AIRS surface emissivity retrievals was calculated over the Sahara Desert, Greenland, and the ARM SGP site. The differences have an effect on the OLR of less than 1.5 W/m^2 with standard deviations on the same order. The day and night differences are not statistically significant in this small number of cases and warrant further study.

[30] AIRS surface temperature retrievals have reported difficulties over deserts, and a 1K error can lead to changes in the OLR of 1 to 2 W/m^2. *Huang and Loeb* [2009] have shown in unpublished work that differences in AIRS and CERES radiances over desert regions are in good agreement, suggesting that something else accounts for the observed bias in OLR. These differences warrant careful examination in future versions of the AIRS level 2 product derived from observed radiances. *Hulley et al.* [2009] in recent results indicate that the mean, absolute daytime land surface emissivity (LSE) difference between AIRS version 5 and the laboratory results for six wavelengths in window regions between 3.9 and 11.4 μm (2564–877 cm^{-1}) was 2.3% over the Namib and 0.70% over the Kalahari with considerable variability for the shorter wavelengths.

[31] The assessment of clear-sky satellite observations over snow and ice covered surfaces have the additional complication of cloud identification which complicates the interpretation of the CERES minus AIRS RRTM OLR comparison. In particular, the land class 15 (Permanent Snow/Ice) shows an agreement of 0.7 W/m^2 during the daytime and >6 W/m^2 at nighttime. Note that the identification of clear sky used in this analysis uses the CERES team method that relies on the MODIS cloud mask which is much more accurate under daytime conditions in the polar regions than at night when the solar reflected channels cannot used and thermal contrast is the primary test [*Frey et al.*, 2008]. In the polar regions, clouds tend to be warmer than the surface skin temperature so that cloud contamination in the CERES clear-sky product would elevate the CERES OLR over the clear-sky estimate of modeled OLR produced by the AIRS RRTM calculation using AIRS cloud cleared radiances as input, leading to the observed positive bias. From this study, it is concluded that the comparison of CERES and AIRS RRTM clear-sky OLR over cold snow and ice surfaces is suspect at night and no firm conclusions can be drawn from the nighttime comparisons. However, the comparisons over snow and ice covered surfaces should be valid in the daytime and classes 15, 18–20 give CERES minus AIRS RRTM biases of 0.7, 0.9, −0.5, and −1.2 W/m^2, respectively, which is quite good agreement.

5. Conclusions

[32] Clear-sky OLR was computed using the AER, Inc. RRTM for comparison with observations from CERES for both ocean and land scenes.

[33] For over 2.5 years at the ARM SGP site, RRTM model calculations of clear-sky OLR using the Best Estimate radiosondes were validated against CERES observations within 0.2% accuracy (CERES minus Best Estimate RRTM bias of −0.05 W/m^2 for daytime, +0.5 W/m^2 for nighttime). The use of AIRS retrieved profiles in RRTM calculations made at the ARM SGP site led to a bias of 0.8% (+0.3 W/m^2 for daytime, and +2.0 W/m^2 for nighttime). The scatter in the biases from the RRTM calculations using AIRS was considerably less than the scatter in calculations using Best Estimate radiosondes (standard deviations of ~2.3 W/m^2 and ~3.6 W/m^2). Replacing the Best Estimate point estimates of surface temperature and unit emissivity with the coincident AIRS skin temperature and emissivity retrieval was shown to reduce the daytime variability to the same value as the CERES minus AIRS RRTM result. The day - night bias (daytime biases minus nighttime biases) was

−0.6 W/m^2 when using Best Estimate RRTM calculations which is less than the uncertainty in the bias estimate (0.7 W/m^2). The day - night bias when using AIRS RRTM calculations (−1.7 W/m^2) was twice as large as the uncertainty at the 95% confidence level.

[34] A partial flux analysis using AIRS radiances at the ARM SGP site implies an accuracy for the RRTM model in the far infrared of 0.4% (about 0.5 W/m^2) for wave numbers less than 650 cm^{-1} (wavelengths greater than 15.4 μm). The mid-infrared region covered by the AIRS spectral radiances is shown to contribute an uncertainty of 0.3% (about 0.4 W/m^2) to the total CERES minus Best Estimate RRTM OLR uncertainty (0.2%).

[35] The comparison of CERES observations with global AIRS RRTM calculations were made for four study days. CERES minus AIRS RRTM comparisons for ocean only clear sky show a bias in the range of +1.0 to +1.6 W/m^2 in the tropics and about +0.8 W/m^2 for midlatitude zones. CERES minus model biases over ocean are similar to previously published results [*Dessler et al.*, 2008; *Huang et al.*, 2008]. Ordering the results according to the magnitude of the measured minus model mean bias for nighttime, tropical, ocean gives: +0.57 ± 1.9 (Dessler/Fu-Liou), +0.83 ± 1.5 (Huang/MODTRAN5), +1.6 ± 1.6 (Moy/RRTM), +3.7 ± 2.1 (Dessler/Chou). The CERES minus AIRS RRTM bias is about 0.8 W/m^2 higher than the CERES minus Huang/MODTRAN5 bias where *Huang et al.* [2008] fit the AIRS radiances directly using MODTRAN. The CERES minus AIRS RRTM bias is about 1.0 W/m^2 higher (2.1 W/m^2 lower) than the Fu-Liou (Chou) model results reported by *Dessler et al.* [2008]. Since the same AIRS profile retrievals were used as input by *Dessler et al.* [2008] this implies a systematic bias in the flux calculation models with RRTM falling between the Fu-Liou and the Chou model. Further validation of clear-sky models for OLR to reduce the uncertainty in the models to the 0.2% level found with RRTM at the ARM SGP site is warranted.

[36] Excluding non-frozen ocean, a mean CERES minus AIRS RRTM difference over land of +2.0 W/m^2 was found for nighttime cases and +1.0 W/m^2 for daytime cases where the land classes are weighted inversely by their standard error. The nighttime bias is quite consistent across all the land classes. The daytime bias shows less consistency with a tendency toward larger CERES minus AIRS RRTM OLR bias for the land classes with smaller vegetation fraction.

[37] Comparison of clear-sky CERES and AIRS RRTM OLR over cold snow/ice covered surfaces (mainly in the polar regions) is complicated by the use of the MODIS cloud mask in the identification of the clear CERES footprints used in the comparison. Clear scenes over cold surfaces can be identified more reliably in the daytime, for which the comparison between CERES and AIRS RRTM is better than 1.2 W/m^2 indicating good agreement. No conclusions can be drawn from the nighttime comparison over cold snow/ice surfaces due to the potential of warm cloud contamination in the CERES clear-sky data set.

[38] **Acknowledgments.** This research was supported by the Office of Biological and Environmental Research of the U.S. Department of Energy under grant DE-FG02-90ER61057 and the National Aeronautics and Space Administration under grant NNX07AD82G.

References

Ackerman, T. P., and G. M. Stokes (2003), The Atmospheric Radiation Measurement program, *Phys. Today*, *56*, 38–45, doi:10.1063/1.1554135.

Aumann, H. H., et al. (2003), AIRS/AMSU/HSB on the Aqua Mission: Design, science objectives, data products, and processing systems, *IEEE Trans. Geosci. Remote Sens.*, *41*, 253–264, doi:10.1109/TGRS.2002.808356.

Aumann, H. H., S. Broberg, D. Elliott, S. Gaiser, and D. Gregorich (2006), Three years of Atmospheric Infrared Sounder radiometric calibration validation using sea surface temperatures, *J. Geophys. Res.*, *111*, D16S90, doi:10.1029/2005JD006822.

Barkstrom, B., E. F. Harrison, G. L. Smith, R. N. Green, J. Kibler, R. Cess, and ERBE Science Team (1989), Earth Radiation Budget Experiment (ERBE) archival and April 1985 results, *Bull. Am. Meteorol. Soc.*, *70*, 1254–1262, doi:10.1175/1520-0477(1989)070<1254:ERBEAA>2.0.CO;2.

Berk, A., et al. (2005), MODTRAN 5: A reformulated atmospheric band model with auxiliary species and practical multiple scattering options: Update, *Proc. SPIE Int. Soc. Opt. Eng.*, *5806*, 662, doi:10.1117/12.606026.

Briegleb, B. P. (1992), Longwave band model for thermal radiation in climate studies, *J. Geophys. Res.*, *97*, 11,475–11,485.

Chahine, M. T. (1977), Remote sounding of cloudy atmospheres. II. Multiple cloud formations, *J. Atmos. Sci.*, *34*, 744–757, doi:10.1175/1520-0469(1977)034<0744:RSOCAI>2.0.CO;2.

Chahine, M. T., et al. (2006), AIRS: Improving weather forecasting and providing new data on greenhouse gases, *Bull. Am. Meteorol. Soc.*, *87*, 911–926, doi:10.1175/BAMS-87-7-911.

Chou, M. D., M. Suarez, X. Z. Liange, and M. M. H. Yan (2001), A thermal infrared radiation parameterization for atmospheric studies, *NASA/TM-2001-104606*, 68 pp., NASA Goddard Space Flight Cent., Greenbelt, Md.

Clough, S. A., F. X. Kneizys, and R. W. Davies (1989), Line shape and the water vapor continuum, *Atmos. Res.*, *23*, 229–241, doi:10.1016/0169-8095(89)90020-3.

Clough, S. A., M. J. Iacono, and J.-L. Moncet (1992), Line-by-line calculation of atmospheric fluxes and cooling rates: 1. Application to water vapor, *J. Geophys. Res.*, *97*, 15,761–15,785.

Clough, S. A., M. W. Shephard, E. Mlawer, J. S. Delamere, M. Iacono, K. Cady-Pereira, S. Boukabara, and P. D. Brown (2005), Atmospheric radiative transfer modeling: A summary of the AER codes, *J. Quant. Spectrosc. Radiat. Transfer*, *91*, 233–244, doi:10.1016/j.jqsrt.2004.05.058.

Dessler, A. E., P. Yang, J. Lee, J. Solbrig, Z. Zhang, and K. Minschwaner (2008), An analysis of the dependence of clear-sky top-of-atmosphere outgoing longwave radiation on atmospheric temperature and water vapor, *J. Geophys. Res.*, *113*, D17102, doi:10.1029/2008JD010137.

Dethof, A., A. Geer, W. Lahoz, F. Goutail, A. Bazureau, D. Y. Wang, and T. von Clarmann (2004), MIPAS Temperature Validation by the MASI Group, *ESA SP-562*, pp. 23.1–23.5, Eur. Space Agency, Paris.

Divakarla, M. G., C. D. Barnet, M. D. Goldberg, L. M. McMillin, E. Maddy, W. Wolf, L. Zhou, and X. Liu (2006), Validation of Atmospheric Infrared Sounder temperature and water vapor retrievals with matched radiosonde measurements and forecasts, *J. Geophys. Res.*, *111*, D09S15, doi:10.1029/2005JD006116.

Frey, R. A., S. A. Ackerman, Y. Liu, K. I. Strabala, H. Zhang, J. R. Key, and X. Wang (2008), Cloud detection with MODIS. Part I: Improvements in the MODIS cloud mask for collection 5, *J. Atmos. Oceanic Technol.*, *25*, 1057–1072, doi:10.1175/2008JTECHA1052.1.

Geier, E. B., R. N. Green, D. P. Kratz, P. Minnis, W. F. Miller, S. K. Nolan, and C. B. Franklin (2003), Clouds and the Earth's Radiant Energy System (CERES) data management system single satellite footprint TOA/surface fluxes and clouds (SSF), SSF_CG_R2V1, NASA Langley Res. Cent., Hampton, Va. (Available at http://science.larc.nasa.gov/ceres/collect_guide/pdf/SSF_CG_R2V1.pdf)

Harrison, E. F., P. Minnis, B. R. Barkstrom, V. Ramanathan, R. D. Cess, and G. G. Gibson (1990), Seasonal variation of cloud radiative forcing derived from the Earth Radiation Budget Experiment, *J. Geophys. Res.*, *95*, 18,687–18,703, doi:10.1029/JD095iD11p18687.

House, F. B. (1985), Observing the earth radiation budget from satellites: Past, present and a look to the future, *Adv. Space Res.*, *5*, 89–98, doi:10.1016/0273-1177(85)90305-9.

Huang, X., and N. Loeb (2009), A consistency check of AIRS and CERES radiances on Aqua, paper presented at 2009 Spring CERES Science Team Meeting, NASA, Newport News, Va.

Huang, X., W. Yang, N. G. Loeb, and V. Ramaswamy (2008), Spectrally resolved fluxes derived from collocated AIRS and CERES measurements and their application in model evaluation: Clear sky over the tropical oceans, *J. Geophys. Res.*, *113*, D09110, doi:10.1029/2007JD009219.

Huang, Y., V. Ramaswamy, and B. Soden (2007), An investigation of the sensitivity of the clear-sky outgoing longwave radiation to atmospheric

temperature and water vapor, *J. Geophys. Res.*, *112*, D05104, doi:10.1029/2005JD006906.

Hulley, G. C., S. J. Hook, E. Manning, S.-Y. Lee, and E. Fetzer (2009), Validation of the Atmospheric Infrared Sounder (AIRS) version 5 land surface emissivity product over the Namib and Kalahari deserts, *J. Geophys. Res.*, *114*, D19104, doi:10.1029/2009JD012351.

Iacono, M. J., E. J. Mlawer, S. A. Clough, and J.-J. Morcrette (2000), Impact of an improved longwave radiation model, RRTM, on the energy budget and thermodynamic properties of the NCAR community climate mode, CCM3, *J. Geophys. Res.*, *105*, 14,873–14,890, doi:10.1029/2000JD900091.

Klaes, K. D., et al. (2007), An introduction to the EUMETSAT Polar System, *Bull. Am. Meteorol. Soc.*, *88*, 1085–1096, doi:10.1175/BAMS-88-7-1085.

Knuteson, R. O., et al. (2004), Atmospheric emitted radiance interferometer. part II: Instrument performance, *J. Atmos. Oceanic Technol.*, *21*, 1777–1789, doi:10.1175/JTECH-1663.1.

Lambin, E. F., and H. J. Geist (Eds.) (2006), *Land-Use and Land-Cover Change. Local Processes and Global Impacts*, 222 pp., Springer, Berlin.

Loeb, N. G., S. Kato, K. Loukachine, N. Manalo-Smith, and D. R. Doelling (2007), Angular distribution models for top-of-atmosphere radiative flux estimation from the Clouds and the Earth's Radiant Energy System instrument on the Terra satellite. Part II: Validation, *J. Atmos. Oceanic Technol.*, *24*, 564–584, doi:10.1175/JTECH1983.1.

McMillin, L. M., J. Zhao, M. K. Rama Varma Raja, S. I. Gutman, and J. G. Yoe (2007), Radiosonde humidity corrections and potential Atmospheric Infrared Sounder moisture accuracy, *J. Geophys. Res.*, *112*, D13S90, doi:10.1029/2005JD006109.

Miloshevich, L. M., H. Vömel, D. N. Whiteman, B. M. Lesht, F. J. Schmidlin, and F. Russo (2006), Absolute accuracy of water vapor measurements from six operational radiosonde types launched during AWEX-G and implications for AIRS validation, *J. Geophys. Res.*, *111*, D09S10, doi:10.1029/2005JD006083.

Minnis, P., and M. M. Khaiyer (2000), Anisotropy of land surface skin temperature derived from satellite data, *J. Appl. Meteorol.*, *39*, 1117–1129, doi:10.1175/1520-0450(2000)039<1117:AOLSST>2.0.CO;2.

Minnis, P., A. V. Gambheer, and D. R. Doelling (2004), Azimuthal anisotropy of longwave and infrared window radiances from the Clouds and the Earth's Radiant Energy System on the Tropical Rainfall Measuring Mission and Terra satellites, *J. Geophys. Res.*, *109*, D08202, doi:10.1029/2003JD004471.

Mlawer, E. J., S. J. Taubman, P. D. Brown, M. J. Iacono, and S. A. Clough (1997), Radiative transfer for inhomogeneous atmospheres: RRTM, a validated correlated-k model for the longwave, *J. Geophys. Res.*, *102*, 16,663–16,682, doi:10.1029/97JD00237.

Mlynczak, M. G., et al. (2006), First light from the Far-Infrared Spectroscopy of the Troposphere (FIRST) instrument, *Geophys. Res. Lett.*, *33*, L07704, doi:10.1029/2005GL025114.

Morcrette, J.-J. (2001), Impact of the radiation-transfer scheme RRTM in the ECMWF forecasting system, *ECMWF Newsl.*, *91*, 2-9.

Pinheiro, A., C. Prigent, and W. Rossow (2008), International Workshop on the Retrieval and Use of Land Surface Temperature: Bridging the Gaps: Summary report, technical report, Natl. Clim. Data Cent., Asheville, N. C.

Raja, M. K. R. V., S. I. Gutman, J. G. Yoe, L. M. McMillin, and J. Zhao (2008), The Validation of AIRS retrievals of integrated precipitable water vapor using measurements from a network of ground-based GPS receivers over the contiguous United States, *J. Atmos. Oceanic Technol.*, *25*, 416–428, doi:10.1175/2007JTECHA889.1.

Revercomb, H. E., D. D. LaPorte, W. L. Smith, H. Buijs, D. G. Murcray, F. J. Murcray, and L. A. Sromovsky (1988), High-Altitude Aircraft Measurements of Upwelling IR Radiance: Prelude to FTIR from Geosynchronous Satellite, *Microchim. Acta*, *95*, 439–444, doi:10.1007/BF01349804.

Revercomb, H. E., et al. (2003), The ARM program's water vapor intensive observation periods—Overview, initial accomplishments, and future challenges, *Bull. Am. Meteorol. Soc.*, *84*, 217–236, doi:10.1175/BAMS-84-2-217.

Rothman, L.S., et al. (2005), The HITRAN 2004 molecular spectroscopic database, *J. Quant. Spectrosc. Radiat. Transfer*, *96*, 139–204, doi:10.1016/j.jqsrt.2004.10.008.

Rutan, D. A., F. G. Rose, N. M. Smith, and T. P. Charlock (2001), Validation data set for CERES surface and atmospheric radiation budget (SARB), *WCRP/GEWEX Newsl.*, *11*, 11-12.

Shephard, M. W., S. A. Clough, V. H. Payne, W. L. Smith, S. Kireev, and K. E. Cady-Pereira (2009), Performance of the line-by-line radiative transfer model (LBLRTM) for temperature and species retrievals: IASI case studies from JAIVEx, *Atmos. Chem. Phys. Discuss.*, *9*, 9313–9366, doi:10.5194/acpd-9-9313-2009.

Sohn, B.-J., and R. Bennartz (2008), Contribution of water vapor to observational estimates of longwave cloud radiative forcing, *J. Geophys. Res.*, *113*, D20107, doi.10.1029/2008JD010053.

Stockton, D., C. Hoffman, J. M. Haas, and C. S. Nelson (2008), The National Polar-Orbiting Operational Environmental Satellite System (NPOESS): Improved capabilities for weather forecasting and environmental monitoring, paper presented at IGARSS 2008, IEEE, Boston, Mass.

Stokes, G. M., and S. E. Schwartz (1994), The Atmospheric Radiation Measurement (Arm) Program: Programmatic background and design of the cloud and radiation test bed, *Bull. Am. Meteorol. Soc.*, *75*, 1201–1221, doi:10.1175/1520-0477(1994)075<1201:TARMPP>2.0.CO;2.

Strow, L. L., S. E. Hannon, S. De-Souza Machado, H. E. Motteler, and D. C. Tobin (2006), Validation of the Atmospheric Infrared Sounder radiative transfer algorithm, *J. Geophys. Res.*, *111*, D09S06, doi:10.1029/2005JD006146.

Susskind, J. (2007), Improved soundings and error estimates from analysis of AIRS/AMSU data, paper presented at SPIE Symposium on Atmospheric and Environmental Remote Sensing Data Processing and Utilization III: Readiness for GEOSS, SPIE, San Diego Calif.

Susskind, J., et al. (2003), Retrieval of atmospheric and surface parameters from AIRS/AMSU/HSB data in the presence of clouds, *IEEE Trans. Geosci. Remote Sens.*, *41*, 390–409, doi:10.1109/TGRS.2002.808236.

Susskind, J., C. Barnet, J. Blaisdell, L. Iredell, F. Keita, L. Kouvaris, G. Molnar, and M. Chahine (2006), Accuracy of geophysical parameters derived from Atmospheric Infrared Sounder/Advanced Microwave Sounding Unit as a function of fractional cloud cover, *J. Geophys. Res.*, *111*, D09S17, doi:10.1029/2005JD006272.

Susskind, J., J. Blaisdell, L. Iredell, and F. Keita (2010), Improved soundings and quality control using AIRS/AMSU data, *IEEE Trans. Geosci. Remote Sens.*, in press.

Tjemkes, S. A., et al. (2003), The ISSWG line-by-line inter-comparison experiment, *J. Quant. Spectrosc. Radiat. Transfer*, *77*, 433–453, doi:10.1016/S0022-4073(02)00174-7.

Tobin, D. C., et al. (1999), Downwelling spectral radiance observations at the SHEBA ice station: Water vapor continuum measurements from 17 to 26 μm, *J. Geophys. Res.*, *104*, 2081–2092, doi:10.1029/1998JD200057.

Tobin, D. C., H. E. Revercomb, R. O. Knuteson, B. M. Lesht, L. L. Strow, S. E. Hannon, W. F. Feltz, L. A. Moy, E. J. Fetzer, and T. S. Cress (2006), Atmospheric Radiation Measurement site atmospheric state best estimates for Atmospheric Infrared Sounder temperature and water vapor retrieval validation, *J. Geophys. Res.*, *111*, D09S14, doi:10.1029/2005JD006103.

Turner, D. D., et al. (2004), The QME AERI LBLRTM: A closure experiment for downwelling high spectral resolution infrared radiance, *J. Atmos. Sci.*, *61*, 2657–2675, doi:10.1175/JAS3300.1.

U.S. Government Printing Office (1976), *U.S. Standard Atmosphere*, Washington, D. C.

Vonder Haar, T. H., and V. Suomi (1971), Measurements of the Earth's radiation budget from satellites during a 5-year period: 1. Extended time and space means, *J. Atmos. Sci.*, *28*, 305–314, doi:10.1175/1520-0469(1971)028<0305:MOTERB>2.0.CO;2.

Wan, Z. (2008), New refinements and validation of the MODIS land-surface temperature/emissivity products, *Remote Sens. Environ.*, *112*, 59–74, doi:10.1016/j.rse.2006.06.026.

Wielicki, B. A., R. D. Cess, M. D. King, D. A. Randall, and E. F. Harrison (1995), Mission to planet Earth—Role of clouds and radiation in climate, *Bull. Am. Meteorol. Soc.*, *76*, 2125–2153, doi:10.1175/1520-0477(1995)076<2125:MTPERO>2.0.CO;2.

Wielicki, B. A., B. R. Barkstrom, E. F. Harrison, R. B. Lee, G. L. Smith, and J. E. Cooper (1996), Clouds and the Earth's radiant energy system (CERES): An Earth observing system experiment, *Bull. Am. Meteorol. Soc.*, *77*, 853–868, doi:10.1175/1520-0477(1996)077<0853:CATERE>2.0.CO;2.

Wielicki, B. A., et al. (1998), Clouds and the Earth's radiant energy system (CERES): Algorithm overview, *IEEE Trans. Geosci. Remote Sens.*, *36*, 1127–1141, doi:10.1109/36.701020.

L. A. Borg, R. O. Knuteson, L. A. Moy, H. E. Revercomb, and D. C. Tobin, Space Science and Engineering Center, University of Wisconsin-Madison, 1225 W. Dayton St., Madison, WI 53706, USA. (robert.knuteson@ssec.wisc.edu)

J. Susskind, Laboratory for Atmospheres, NASA Goddard Space Flight Center, Greenbelt, MD 20771-0001, USA.